

## EFFECT OF pH ON PHOTOCATALYTIC ACTIVITIES OF BiOBr NANOMATERIALS SYNTHESIZED BY SONOCHEMICAL METHOD

P. PATIPHATPANYA<sup>a,b</sup>, P. INTAPHONG<sup>c</sup>, A. PHURUANGRAT<sup>c\*</sup>,  
B. KUNTALUE<sup>d</sup>, P. DUMRONGROJTHANATH<sup>e</sup>, T. THONGTEM<sup>a,f</sup>,  
S. THONGTEM<sup>f,g</sup>

<sup>a</sup>Department of Chemistry, Faculty of Science, Chiang Mai University,  
Chiang Mai 50200, Thailand

<sup>b</sup>Ph.D. Degree Program in Chemistry, Faculty of Science, Chiang Mai University,  
Chiang Mai 50200, Thailand

<sup>c</sup>Department of Materials Science and Technology, Faculty of Science,  
Prince of Songkla University, Hat Yai, Songkhla 90112, Thailand

<sup>d</sup>Electron Microscopy Research and Service Center, Faculty of Science,  
Chiang Mai University, Chiang Mai 50200, Thailand

<sup>e</sup>Rajamangala University of Technology Lanna Chiang Rai,  
Chiang Rai 57120, Thailand

<sup>f</sup>Materials Science Research Center, Faculty of Science, Chiang Mai University,  
Chiang Mai 50200, Thailand

<sup>g</sup>Department of Physics and Materials Science, Faculty of Science,  
Chiang Mai University, Chiang Mai 50200, Thailand

BiOBr nanomaterials were successfully synthesized in different solutions with the pH of 2–12 by sonochemical method. X-ray diffraction (XRD), scanning electron microscopy (SEM) and X-ray photoelectron spectroscopy (XPS) results revealed the presence of pure tetragonal BiOBr nanomaterials. The photocatalytic activities of BiOBr nanomaterials were evaluated through the degradation of rhodamine B (RhB) under visible light irradiation. Clearly, the pH of precursor solution played an important role in photocatalytic activity. In this research, BiOBr flowers synthesized in a solution with the pH of 6 showed the highest photocatalytic efficiency of 99.05 % within 40 min.

(Received September 8, 2019; Accepted February 13, 2020)

**Keywords:** BiOBr; Sonochemical method; Photocatalysis

### 1. Introduction

Over the last decades, semiconductor photocatalysts can play an important role in degradation of organic/inorganic contaminants and splitting water under solar radiation [1–3]. TiO<sub>2</sub> has been the most use as an excellent photocatalyst because it has a wide band gap of 3.2 eV. Moreover, it has fast rate of recombination of photo-induced electron–hole pairs and absorbs only UV radiation [2–5]. Thus great effort is focused on the development of highly efficient visible-light-driven photocatalyst.

Recently, bismuth oxyhalides (BiOX, X=Cl, Br, I) have become one of the interesting materials in the field of photocatalysis. BiOX materials have layered structure consisting of alternating arranged [Bi<sub>2</sub>O<sub>2</sub>]<sup>2+</sup> mono layer and double layer of X<sup>-</sup> ion along the c-axis, which can be expressed as [X–Bi–O–Bi–X] [5–7]. The layer structure can effectively induce the separation of photo-induced electron–hole pairs and show excellent photocatalytic activity. Among them, BiOBr has band gap energy of 2.3 eV and has good photocatalytic activity under visible light irradiation (48 % of solar radiation) [8].

---

\* Corresponding author: phuruangrat@hotmail.com

There are many methods used to synthesize BiOBr photocatalyst with different kinds of crystalline degree, particle size and morphology. Hydrolysis, hydrothermal, solvothermal and microwave are very interesting synthetic methods [9, 10]. Each of these methods can be operated under different conditions, which can lead to different structures with different photocatalytic activities. Recently, ultrasonic irradiation has been used to synthesize semiconducting photocatalyst. The method can cause physical and chemical changes through audio cavitation such as growth, rapid formation and collapse of unstable bubbles in liquid. This method creates nano-scale particles and requires short preparation time [11].

In this study, BiOBr photocatalyst was prepared by sonochemical method. Effect of pH on phase, morphology and photocatalytic property of BiOBr was investigated by X-ray diffraction (XRD), scanning electron microscopy (SEM) and X-ray photoelectron spectroscopy (XPS). Photocatalytic activity of BiOBr was studied through degradation of rhodamine B (RhB) under visible light irradiation. The pH of precursor solutions played an important role in morphology and photocatalytic activity of BiOBr nanomaterials.

## 2. Experiment

To synthesize BiOBr, 0.01 mole of  $\text{Bi}(\text{NO}_3)_3$  and 0.01 mole of NaBr were dissolved in 100 ml reverse osmosis (RO) water which was stirred to mix the reagents thoroughly. Each of the solutions was adjusted the pH to 2–12 by 3M NaOH. The solutions were ultrasonically processed in a bath at 80 °C for 5 h. The precipitates were collected and dried at 100 °C. The as-synthesized samples were characterized by an X-ray diffractometer (XRD, Philips X'Pert MPD) operating at 20 kV and 15 mA with Cu  $K_\alpha$  in the  $2\theta$  range of  $10^\circ$ – $60^\circ$ . A scanning electron microscope (SEM) was operated by a JEOL JSM 6335F SEM at 15 kV. X-ray photoelectron spectroscopy (XPS) was carried out by an Axis Ultra DLD, Kratos Analytical Ltd XPS using Al  $K_\alpha$  at 1486.6 eV as an excitation source and C 1s at 285.1 eV as a standard.

Each 200 mg of photocatalyst in 200 ml of  $1 \times 10^{-5}$  M RhB solution was used to test for photocatalysis. The suspension was stirred in the dark for 30 min before visible light illumination from a Xe lamp. During photocatalysis, each 5 ml suspension was collected at every time interval and centrifuged. The concentration of RhB was measured at 554 nm by a UV-visible spectrophotometer (Perkin Elmer Lambda 25). The decolorization efficiency was calculated by the equation

$$\text{Decolorization efficiency (\%)} = \frac{C_0 - C_t}{C_0} \times 100 \quad (1)$$

, where  $C_0$  is the initial concentration of RhB and  $C_t$  is the concentration of RhB after visible light irradiation within the elapsed time (t).

## 3. Results and discussion

Fig. 1 shows XRD patterns of BiOBr photocatalysts synthesized in different solutions with the pH of 2, 4, 6, 8, 10 and 12 by a sonochemical method. All diffraction peaks of the samples can be indexed to the tetragonal phase of BiOBr corresponding to the database of JCPDS No. 09-0393 [12]. Moreover, the diffraction peaks of the as-synthesized BiOBr samples are intense and sharp, indicating that the BiOBr products are well-crystallized [13, 14]. No impurity peaks were detected in the XRD patterns. The results indicated that the BiOBr products can be synthesized in the solutions with the pH of 2–12 by a sonochemical method. The intensities of diffraction peaks with the (001) series in the acidic condition at the pH of 2–6 were lessened with the increasing in the pH of the solutions. They show that the samples are anisotropic and grew along the [001] direction which is in accordance with the crystalline BiOBr [15]. Upon further increasing the pH of solutions to be in the range of basic condition, the increasing in the intensities of diffraction peaks of BiOBr became lessened and the diffraction peaks became broadened. The results certified that particle sizes of BiOBr samples were decreased. Clearly, the crystallite size and growth direction

of the BiOBr samples are strongly controlled by the solution pH. Upon decreasing in the pH of solutions in the acidic condition, anisotropic growth of BiOBr is along the [001] direction. The increasing in the pH of solution in basic condition, smaller crystallite size is produced.

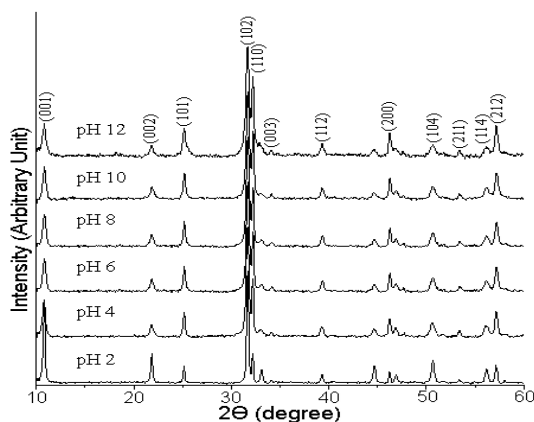


Fig. 1 XRD patterns of BiOBr synthesized in solutions with different pH by sonochemical method.

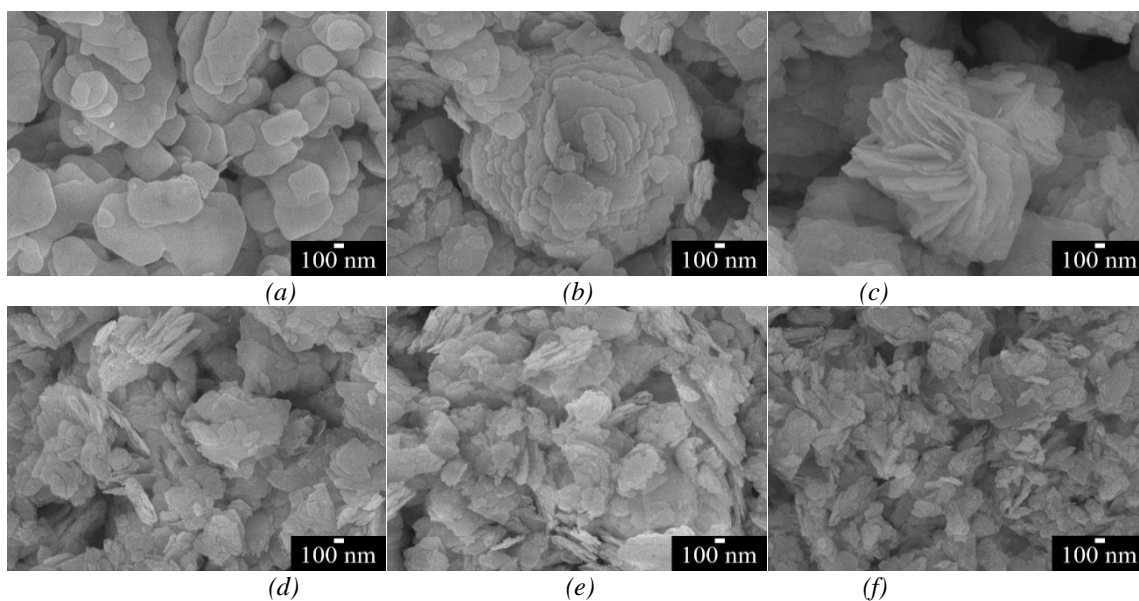


Fig. 2 SEM images of BiOBr synthesized in different solutions with the pH of (a) 2, (b) 4, (c) 6, (d) 8, (e) 10 and (f) 12.

Morphologies of the as-synthesized BiOBr products in different pH were characterized by SEM as the results shown in Fig. 2. It can be seen that BiOBr sample synthesized in the solution with the pH of 2 was composed of only microplates with size of 300–500 nm diameter. At the pH of 4, nanoplate islands formed. The nanoplate islands transformed into assembled flowers of mesoporous hierarchical BiOBr structure at the pH of 6. The flower-like mesoporous hierarchical BiOBr structures are built by connecting each of the nanoplates around a center. In the range of basic condition (pH = 8–12), some petals of flower-like mesoporous hierarchical BiOBr structures were released and formed colonies of BiOBr nanoplates as the results shown in Fig. 2d–f.

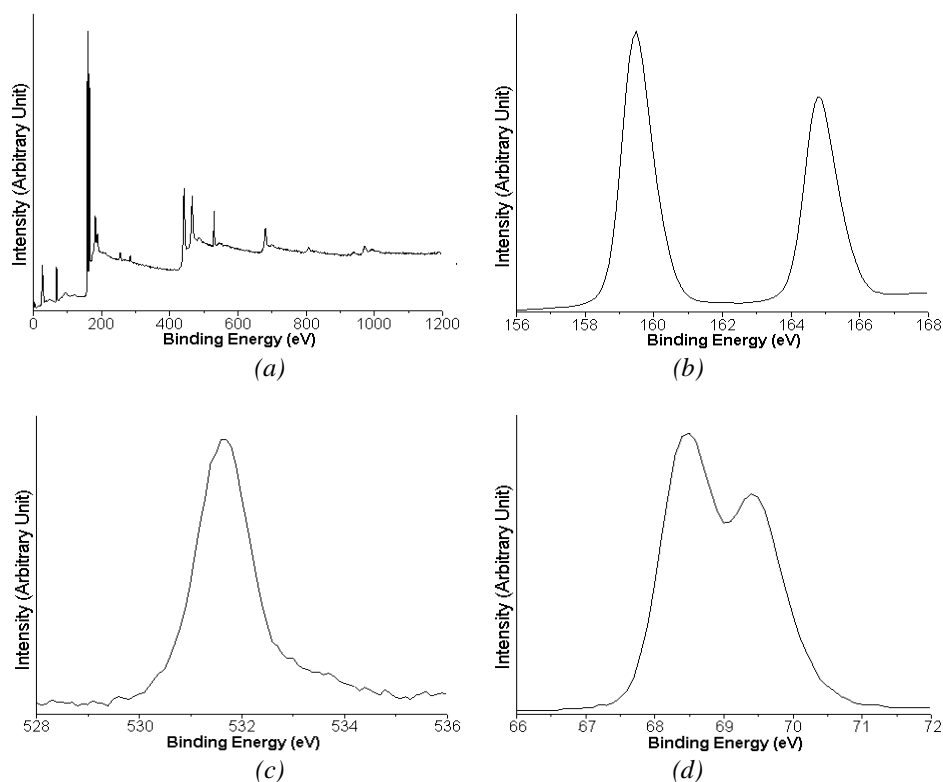


Fig. 3 XPS spectra of (a) full survey scan, (b) Bi 4f, (c) O 1s and (d) Br 3d of BiOBr synthesized in the solution with the pH of 6 by sonochemical method.

The composition and oxidation state of BiOBr synthesized in the solution with the pH of 6 were analyzed by XPS as the results shown in Fig. 3. The full survey XPS spectrum of sample shows the binding energies of Bi, O and Br elements. Clearly, the product is very pure. The high-resolution XPS spectrum of Bi 4f core level shows two binding energy peaks at 159.47 eV and 164.80 eV corresponding to Bi 4f<sub>7/2</sub> and Bi 4f<sub>5/2</sub>, respectively. The results indicate that Bi species in the BiOBr sample are Bi<sup>3+</sup> [15–18]. O 1s shows a binding energy peak at 531.62 eV which is assigned to the Bi–O bonding of [Bi<sub>2</sub>O<sub>2</sub>]<sup>2+</sup> in BiOBr sample [15–18]. The high-resolution XPS spectrum of Br 3d core level shows two binding energy peaks at 68.48 eV and 69.50 eV corresponding to Br 3d<sub>5/2</sub> and Br 3d<sub>3/2</sub>, respectively. These indicate that Br species are Br<sup>−</sup> ions containing in BiOBr sample [15–18].

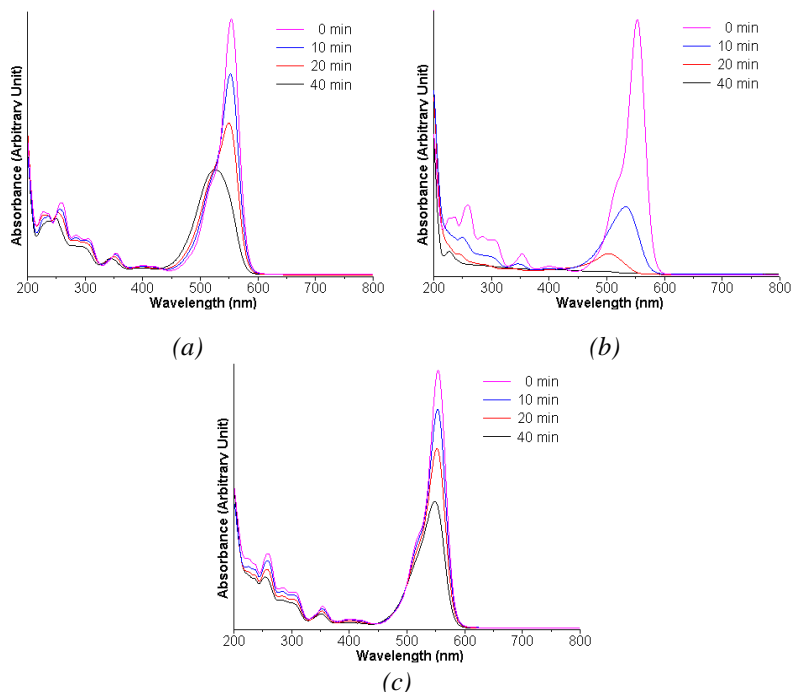


Fig. 4 UV-visible absorption of RhB over BiOBr synthesized in the solutions with the pH of (a) 2, (b) 6 and (c) 12 by sonochemical method.

Photocatalytic activities of the as-synthesized BiOBr samples at different pH via sonochemical method were investigated through photodegradation of RhB under visible light irradiation. Fig. 4 shows the evolution of spectral absorption through the photodegradation of RhB solution by the as-synthesized BiOBr at the pH of 2, 6 and 12 under visible light irradiation. Clearly, RhB solutions with maximum wavelength absorption ( $\lambda_{\max}$ ) at 554 nm over the as-synthesized BiOBr samples show the decrease of  $\lambda_{\max}$  with the temporal evolution of visible light region. Among these three, the UV-visible absorption peak of as-synthesized BiOBr sample at the pH of 6 is the lowest. The results certify that BiOBr synthesized in the solution with the pH of 6 has the highest photodegradation of RhB molecules. At the beginning photocatalysis, pink solution gradually faded to colorless solution within 40 min, suggesting that RhB molecules were completely destroyed. The spectra of RhB were blue-shifted and can be specified as the deethylation process of RhB dye [19, 20]. The resultant N-deethylation of RhB contains N,N,N'-triethyl rhodamine (539 nm), N,N'-diethyl rhodamine (522 nm), N-ethyl rhodamine (510 nm) and rhodamine (498 nm) [21, 22].

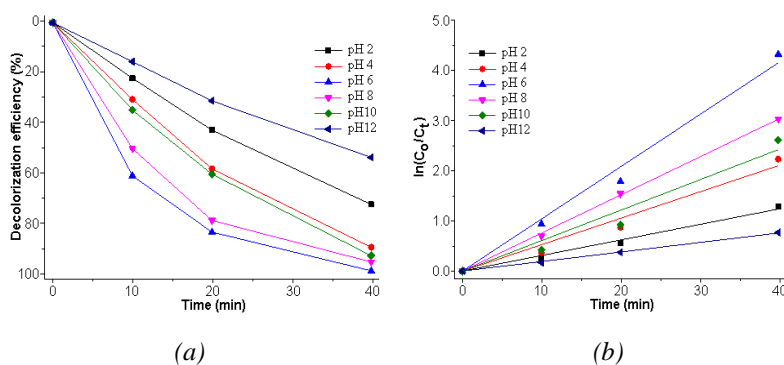
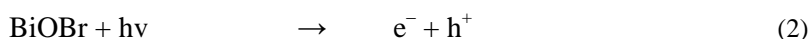


Fig. 5 (a) Decolorization efficiency and (b) pseudo-first-order plot for photocatalytic degradation of RhB by BiOBr synthesized in the solutions with different pH by sonochemical method.

BiOBr photocatalysts prepared in the solutions with different pH by sonochemical method were studied for photocatalytic degradation of RhB under visible light irradiation as the results shown in Fig. 5a. The photodegradation efficiencies of RhB over BiOBr synthesized in the solutions with the pH of 2, 4, 6, 8, 10 and 12 are 73.32 %, 89.32 %, 99.05 %, 95.20 %, 92.70 % and 53.58 % within 40 min, respectively. The photocatalytic efficiency of RhB degradation over BiOBr synthesized in the solution with the pH of 6 has the highest photocatalytic performance because mesoporous hierarchical BiOBr structure has the highest photocatalytic performance. The chemical reactions for photon-assisted generation of electron–hole pairs and subsequent formation of  $\bullet\text{O}_2^-$  and  $\bullet\text{OH}$  radicals are shown below. In the end, dye molecules were degraded into water and carbon dioxide.



An increase in the surface area of BiOBr by forming mesoporous hierarchical BiOBr structure can lead to produce more  $\bullet\text{O}_2^-$  and  $\bullet\text{OH}$  radicals on the surface of BiOBr photocatalyst and to enhance photocatalytic activity [15, 17, 23]. To have better understanding of the reaction kinetics of RhB degradation, the experimental data were fitted to pseudo-first-order simplification of Langmuir–Hinshelwood kinetics, which is well established for photocatalysis at low initial pollutant concentration. The relevant equation is shown below.

$$\ln(C_0/C_t) = k_{\text{app}}t \quad (6)$$

, where  $k_{\text{app}}$  is the apparent first-order rate constant ( $\text{min}^{-1}$ ), obtained by the slopes of the  $\ln(C_0/C_t)$  versus  $t$  plots (Fig. 5b).  $C_0$  and  $C_t$  are the concentrations of dye in solutions at irradiation time of 0 and  $t$ , respectively [21–23]. All photocatalysts obey pseudo-first-order reactions because the plots are very close to the linear trends [20, 24]. In this research, the apparent first-order rate constants of RhB degradation over BiOBr synthesized in the solutions with the pH of 2, 4, 6, 8, 10 and 12 are  $0.0308 \text{ min}^{-1}$ ,  $0.0527 \text{ min}^{-1}$ ,  $0.1040 \text{ min}^{-1}$ ,  $0.0755 \text{ min}^{-1}$ ,  $0.0606 \text{ min}^{-1}$  and  $0.0186 \text{ min}^{-1}$  under visible light irradiation within 40 min, respectively. BiOBr synthesized in the solution with the pH of 6 has the highest apparent rate constant and the highest photocatalytic rate for degradation of RhB solution under visible light irradiation.

The stability and repeatability of the photocatalyst are the important parameters for performance evaluation. For each photocatalytic experiment, the photocatalyst was centrifuged, washed with distilled water and ethanol, and dried at  $100 \text{ }^\circ\text{C}$  for 24 h. Photocatalytic results of the recycled BiOBr sample are shown in Fig. 6. In this research, the degradation rate of RhB at the end of the 5<sup>th</sup> recycled test was 97.50 %. The result certifies that the as-synthesized BiOBr is good photocatalytic repeatability.

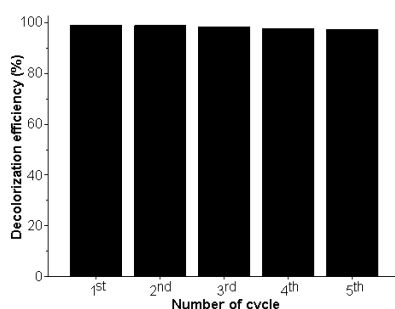


Fig. 6 Recyclability for photodegradation of RhB by BiOBr synthesized in the solution with the pH of 6 by sonochemical method.

#### 4. Conclusions

BiOBr photocatalysts were successfully synthesized in different solutions with the pH of 2, 4, 6, 8, 10 and 12 by sonochemical method. The assembled flowers of mesoporous hierarchical BiOBr structure obtained in the solution with the pH of 6 have the highest photodegradation of RhB of 99.05 % within 40 min and are stable and repeatable in the RhB solution under visible light irradiation.

#### Acknowledgement

We are extremely grateful to Prince of Songkla University, Hat Yai, Songkhla 90112, Thailand for providing financial support.

#### References

- [1] H. Li, J. Liu, T. Hu, N. Du, S. Song, W. Hou, *Mater. Res. Bull.* **77**, 171 (2016).
- [2] Z. Liu, B. Wu, *Mat. Sci. Semicon. Proc.* **31**, 68(2015).
- [3] J. Cao, B. Xu, B. Luo, H. Lin, S. Chen, *Catal. Commun.* **13**, 63 (2011).
- [4] Y. Huo, J. Zhang, M. Miao, Y. Jin, *Appl Catal. B* **111-112**, 344 (2012).
- [5] G. Jiang, X. Li, Z. Wei, T. Jiang, X. Du, W. Chen, *Powder Technol.* **260**, 84 (2014).
- [6] T. Yan, X. Yan, R. Guo, W. Zhang, W. Li, J. You, *Catal. Commun.* **42**, 30 (2013).
- [7] Y. Feng, L. Li, J. Li, J. Wang, L. Liu, *J. Hazard. Mater.* **192**, 538 (2011).
- [8] Z. Jiang, F. Yang, G. Yang, L. Kong, M. O. Jones, T. Xiao, P. P. Edwards, *J. Photoch. Photobio. A* **212**, 8 (2010).
- [9] C. Deng, H. Guan, *Mater. Lett.* **107**, 119 (2013).
- [10] L. Zhang, X. Cao, X. Chen, Z. Xue, *J. Colloid. Interf. Sci.* **354**, 630 (2011).
- [11] C. Yang, F. Li, T. Li, W. Cao, *J. Mol. Catal. A* **418-419**, 132 (2016).
- [12] Powder Diffract. File, JCPDS-ICDD, 12 Campus Bld., Newtown Square, PA 19073-3273, U.S.A. (2001).
- [13] X. Xiong, L. Ding, Q. Wang, Y. Li, Q. Jiang, J. Hu, *Appl. Catal. B* **188**, 283 (2016).
- [14] H. Li, T. Hu, J. Liu, S. Song, N. Du, R. Zhang, W. Hou, *Appl. Catal. B* **182**, 431 (2016).
- [15] Z. Liu, B. Wu, Y. Zhao, J. Niu, Y. Zhu, *Ceram. Int.* **40**, 5597 (2014).
- [16] L. Lu, L. Kong, Z. Jiang, H.H.C. Lai, T. Xiao, P. P. Edwards, *Catal. Lett.* **142**, 771 (2012).
- [17] J. Han, G. Li, L. Qiang, X. Zhai, C. Jiang, *J. Mater. Sci.* **30**, 5995 (2019).
- [18] Z. Zhang, Y. Wang, X. Zhang, C. Zhang, Y. Wang, H. Zhang, C. Fan, *Chem. Pap.* **72**, 2413 (2018).
- [19] M. He, W. Li, J. Xia, L. Xu, J. Di, H. Xu, S. Yin, H. Li, M. Li, *Appl. Surf. Sci.* **331**, 170 (2015).
- [20] Y. Zhao, X. Tan, T. Yu, S. Wang, *Mater. Lett.* **164**, 243 (2016).
- [21] P. Intaphong, A. Phuruangrat, K. Karthik, T. Thongtem, S. Thongtem, *Digest J. Nanomater. Biostr.* **14**, 593 (2019).
- [22] S. Sitthichai, S. Jonjana, A. Phuruangrat, B. Kuntalue, T. Thongtem, S. Thongtem, *J. Ceram. Soc. Japan* **125**, 387 (2017).
- [23] P. Intaphong, A. Phuruangrat, S. Thongtem, T. Thongtem, *Digest J. Nanomater. Biostr.* **13**, 177 (2018).
- [24] L. Lu, M. Zhou, Lu Yin, G. Zhou, T. Jiang, X. Wan, H. Shi, *J. Mol. Catal. A* **423**, 379 (2016).